ISBN: 978-3-95450-205-9 doi:10.18429/JACoW-Cyclotrons2019-TUB03

MRI-GUIDED-PT: INTEGRATING AN MRI IN A PROTON THERAPY SYSTEM

E. van der Kraaij†, J. Smeets, Ion Beam Applications S.A., 1348 Louvain-la-Neuve, Belgium
L. Bertora, A. Carrozzi, A. Serra, ASG Superconductors S.p.A., 16152 Genova, Italy
B. Oborn, Centre for Medical Radiation Physics (CMRP),
University of Wollongong, Wollongong, NSW 2500, Australia
S. Gantz, A. Hoffmann, L. Karsch, A. Lühr, J. Pawelke, S. Schellhammer
OncoRay – National Center for Radiation Research in Oncology, Faculty of Medicine and
University Hospital Carl Gustav Carus, Technische Universität Dresden,
Helmholtz-Zentrum Dresden – Rossendorf, Dresden 01307, Germany

Abstract

Integration of magnetic resonance imaging (MRI) in proton therapy (PT) has the potential to improve tumor-targeting precision. However, it is technically challenging to integrate an MRI scanner at the beam isocenter of a PT system due to space constraints and electromagnetic interactions between the two systems. We present a concept for the mechanical integration of a 0.5 T MRI scanner (MR-Open, ASG Superconductors) into a PT gantry (ProteusONE, IBA). Finite element modelling (FEM) simulations are used to assess the perturbation of several of the gantry's elements on the homogeneity of the scanner's static magnetic field. Results show that only the perturbations by the bending magnet are significant and to be taken into account during treatment planning and dose delivery.

INTRODUCTION

Image guidance in conventional PT systems is provided by X-ray or (cone-beam) CT systems. Better image guidance and adaptive therapies for several tumor sites can be achieved by changing to MRI guidance. The first benefit of MRI is the absence of ionizing radiation dose: an advantage in for example paediatric cases and an enabler for continuous imaging. Daily adaptations of the treatment plan and organ motion visualization in for example the abdomen or the thorax become feasible. Secondly, MRI provides unparalleled soft-tissue contrast, enabling margin reduction in the treatment planning and potentially hypo-fractionation. For more information and an overview of the subject the reader is referred to [1].

Challenges

Before an MRI-guided-PT system can be designed there are several technical challenges to overcome. We mention the four most pressing issues. Firstly, there is the problem how to mechanically integrate the two large complex devices. Secondly, there is the mutual magnetic interference to be taken into account: the perturbation of the image quality by the PT system and the perturbation of the beam quality by the MRI's magnetic fields. Thirdly, there is the integration of a Faraday cage to shield the MRI from surrounding RF sources and it needs to be confirmed that the MRI receiver coils function correctly in or near the beam path, without altering the beam properties. Finally, methods for dosimetry in the presence of a magnetic field need to be established. All of this, and more, requires adjustment of the treatment workflow for a synchronized operation of both the imaging and the treatment equipment.

Scope of Proceedings

In these proceedings we discuss the mechanical integration of an MRI scanner on a PT gantry and an FEM study to assess the perturbation of the gantry's elements on the homogeneity of the MRI scanner's magnetic field.

A PT gantry comprises strong magnets mounted on heavy, ferromagnetic, iron support structures. These can be detrimental to the B-field homogeneity of an MRI scanner. Two possible sources of perturbation are studied. Firstly, the gantry rotation: Moving ferromagnetic objects can cause a change in the B-field. Secondly, the magnetic fringe field of the 60° bending magnet on the gantry: This last magnet on the gantry is closest to the MRI scanner and has a field that varies with beam energy.

Further Research

To test the technical feasibility, a first experimental set-up was realized at the PT center in Dresden, combining a 0.22 T open MRI scanner with a static proton beam line. For more information, the reader is referred to [2].

MECHANICAL INTEGRATION

A 0.5 T open MRI scanner is the preferred choice for the integration with an IBA ProteusONE system [3]. The scanner's design would be based on that of the MR-Open manufactured by ASG Superconductors [4], see Fig. 1.

The low field strength scanner is foreseen to provide a good contrast-to-noise ratio and adequate image resolution [5]. At the same time, the liquid helium free scanner is based on a dry-cooled, superconducting magnet and has a large opening for patients between the magnet coils.

By modifying the C-shaped yoke of the MR-Open to a closed yoke, the integration of the MR on the PT system is foreseen as shown in Fig. 2. The beam exiting from the gantry to the isocenter is parallel to the B-field of the MRI

† erik.vanderkraaij@iba-group.com

ISBN: 978-3-95450-205-9 doi:10.18429/JACoW-Cyclotrons2019-TUB03

scanner at isocenter (B_0), assuring the least possible deflection of the proton beam. The beam passes through a hole in the yoke, visible in the blue yoke of Fig. 1 (right).

Figure 1: Left is shown a clinical version of the MR-Open scanner. Right is the MRI yoke with the coil structures.

The structure in Fig. 2 has several benefits: the MRI scanner is coupled to the gantry for simultaneous rotation. The rotating structures can be decoupled for maintenance purpose. The patient opening is large, reducing as much as possible claustrophobic anxieties and giving easy access for QA.

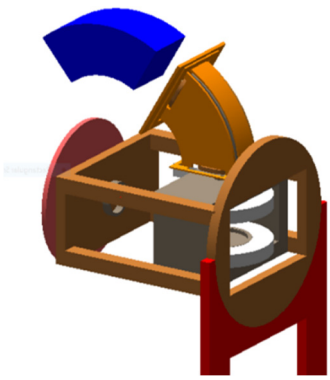

Figure 2: Conceptual drawing of an open MRI scanner mounted at the PT gantry's isocenter. Shown are the gantry's last two bending magnets, the MRI yoke, the MRI coils and support structures.

FINITE ELEMENT ANALYSIS

For the FEM simulations, Opera3D v.18R2x64 was used with its Magnetostatic solver [6]. To ensure mesh independence of the analysis, one large model was created, as depicted in Fig. 3. It contains a slightly simplified model of the gantry, including its counterweight and its last 60° bending magnet, two support structures (the gantry's "chair") and the MRI scanner. Table 1 lists several dimensions of the MRI scanner and gantry. In real life, more ferromagnetic material will surround the system. The gantry's chair is however by far the largest element rotating around the scanner and was thus for now taken as the only rotating perturbation source.

Model Setup

The model has been recreated nine times, with the gantry rotated by -30°, 0°…, 210° relative to the chair[1]. For each angle model, after the meshing, the solver was run with the chair set to either air or iron and the current in the bending magnet was set to 0% or 100% of its maximum value. The MRI coils always had the same current setting.

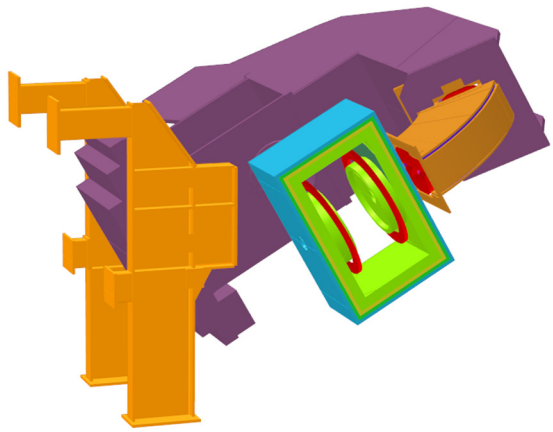

Figure 3: Opera3D model of the gantry (purple), the gantry's chair (orange), the MRI scanner and the 60° bending magnet at isocenter. This model has the gantry and scanner rotated relative to the vertical position by +60°. The scanner model can be seen to consist of several layers, to study different yoke thicknesses.

Table 1: Model Properties as Simulated

Parameter	Value
MRI:	
Pole gap	600 mm
Pole diameter (=depth)	1166 mm
Inner width	2000 mm
Yoke thickness (min - max)	150 - 300 mm
Yoke height (max)	1730 mm
B at isocenter (B_0)	0.53 T
Iron mass (min - max)	13 – 24 ton
PT system:	
Gantry iron mass, incl. 60°-bend	82 ton
Gantry chair iron mass	10 ton
Bending magnet B-field (max)	1.5 T

To study the perturbations on the B-field homogeneity as a function of the MRI scanner's yoke thickness, the inner part of the yoke was always simulated as iron. Three extra layers of 50 mm each were present in all models and the solver was run with these layers set to either air or iron. Thus, the MRI was simulated with different yoke thicknesses of 150, 200, 250 and 300 mm.

Solver Settings

As the calculations are at the ppm level of the magnetic field, the TOSCA 'Nonlinear iteration convergence tolerance' was set to 10^{-6}. A lower setting did not result in better performance.

The integration method for calculations in Opera3D could not be used. In a recent upgrade a stochastic element has been added to this calculation method [7],

[1] The ProteusONE can rotate from 0° up to 220°.

ISBN: 978-3-95450-205-9 doi:10.18429/JACoW-Cyclotrons2019-TUB03

speeding up the calculation, but also introducing a fluctuation. The Field Calculation Method was therefore set to Nodal Interpolation mode.

Legendre Polynomial Fitting

The field homogeneity at isocenter in the MRI scanner was analyzed by fitting for each solved model the Legendre polynomial

$$\frac{(B_z - B_0)}{B_0} \cdot 10^6 = \sum_{n=0}^{N} \sum_{m=0}^{n} P_{nm}(\cos(\theta))[\alpha_{nm} \cos(m\varphi) + \beta_{nm} \sin(m\varphi)]$$

up to N=15, at a radius of 200 mm. Spherical coordinates (r, θ, φ) are used, with z parallel to the beam direction and x along the gantry rotation axis. B_z is the magnetic field in vertical direction. B_0 is defined as B_z at isocenter, for the model at 0° rotation angle, with the yoke fully made of iron and all other elements set to air.

To assure mesh independence, only relative measurements were analyzed: the results with the chair set to iron were subtracted by the results of the chair set to air, and the results with the bend current at 100% were subtracted by those at 0%. In other words, the perturbations were obtained by subtracting coefficient by coefficient:

$$\alpha_{nm}^{\text{pert rot}} = \alpha_{nm}^{\text{chair set to iron}} - \alpha_{nm}^{\text{chair set to air}}$$

and

$$\alpha_{nm}^{\text{pert bend}} = \alpha_{nm}^{\text{bend current 100\%}} - \alpha_{nm}^{\text{bend current 0\%}}.$$

RESULTS

Due to symmetry reasons, almost all β-coefficients are zero. The discussion of the results is therefore mostly on the α-coefficients.

Unfortunately, the angle model of 210° did not converge for all its different settings. The set of 210° is thus not included in the final analysis.

Perturbation by Gantry Rotation

For this perturbation study the current in the gantry's bending magnet was always at 0%.

In Fig. 4 the results are shown for $\alpha_{00}^{\text{pert rot}}$ at different rotation angles. This value is the perturbation effect of the chair on the average of the magnetic field in the MRI scanner as it rotates around the gantry axis. This figure shows the results with the gantry set to air.

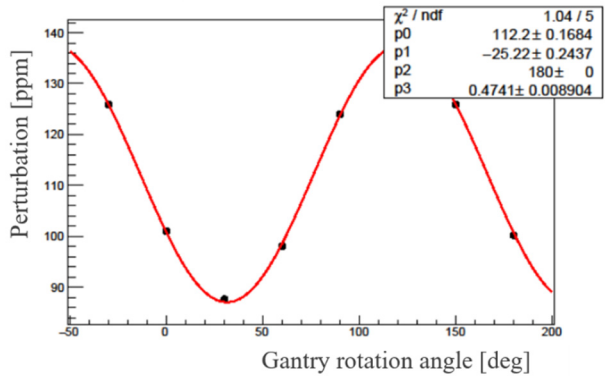

Figure 4: $\alpha_{00}^{\text{pert rot}}$ versus gantry rotation angle.

In the figure, the value at rotation angle 0° is non-zero, as B_0 is defined for the model with the chair and gantry set to air. The average of the figure has thus no significant meaning. It requires only passive compensation and can be compensated by magnet shimming at installation.

The amplitude of the fluctuation of the perturbation in the figure is fitted with a sinusoidal function to 25 ppm. This perturbation amplitude means that over a full rotation around the gantry axis, a maximum shift of ±25 ppm of the average B_z in a sphere of 400 mm diameter at isocenter can be expected.

Repeating the above sinusoidal fit on the set of results with the gantry set to iron and with different MRI yoke thicknesses, the perturbation amplitudes in Fig. 5 were obtained.

Perturbations due to rotation during system operation require active compensation. For $\alpha_{00}^{\text{pert rot}}$, the MRI receiver coil frequency can be adjusted and the maximum of ~45 ppm is easy to adapt to. The $\alpha_{n=1,m}^{\text{pert rot}}$ reflect linear perturbations on the field homogeneity and can be compensated for by the MRI gradient coils. Note that $\alpha_{10}^{\text{pert rot}}$ is along the z-axis and $\alpha_{11}^{\text{pert rot}}$ is along the rotation axis. $\beta_{11}^{\text{pert rot}}$ is perpendicular to both.

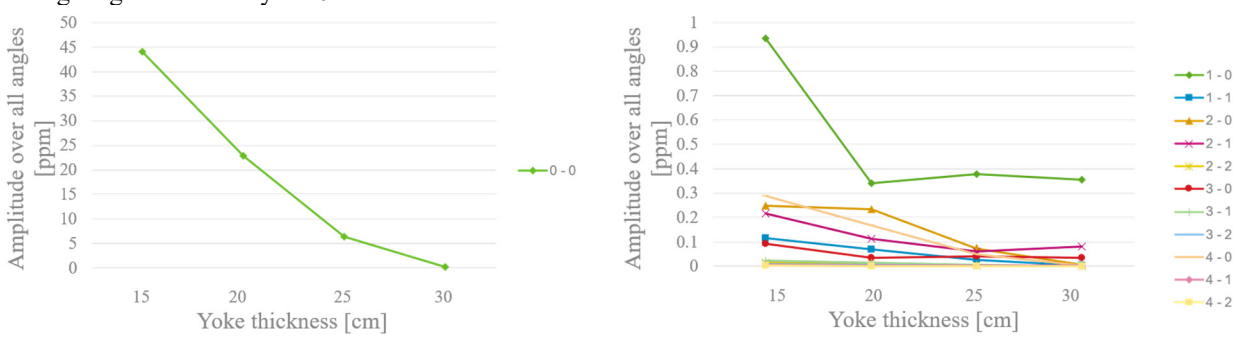

Figure 5: Fitted perturbation amplitudes versus yoke thickness for $\alpha_{00}^{\text{pert rot}}$ (left) and for higher orders with $n \geq 1$ (right). The legends list the $n - m$ parameters.

ISBN: 978-3-95450-205-9 doi:10.18429/JACoW-Cyclotrons2019-TUB03

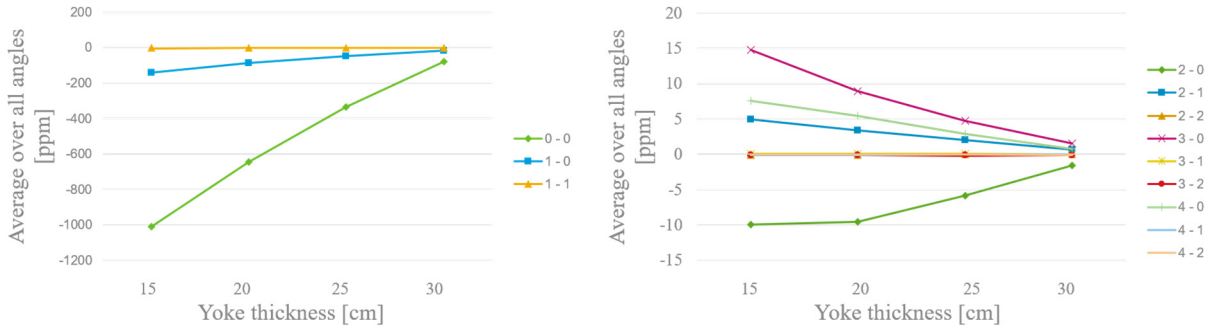

Figure 6: Fitted perturbation averages versus yoke thickness for the first orders of $\alpha_{nm}^{\text{pert bend}}$ (left) and for higher orders with $n \geq 2$ (right). The legends list the $n-m$ parameters.

For the MR-Open, linear adjustments by the gradient coils can be taken care of up to 100 ppm. The higher order perturbations (n ≥ 2) can be seen in Fig. 5 to be below the ppm level and need no compensation.

Perturbation by 60° Bending Magnet

For this perturbation study the gantry and the gantry's chair were all included as iron.

The results for $\alpha_{nm}^{\text{pert bend}}$ versus gantry rotation angle show no significant fluctuation as function of the angle. The average of the perturbations over the angles is therefore studied.

In Fig. 6 the fitted perturbation averages are given for $\alpha_{nm}^{\text{pert bend}}$, with $(n,m) \leq (4,2)$. Higher order perturbations are negligible, i.e. < 1 ppm. In Fig. 7 the fitted perturbation averages are given for the β coefficients.

The lowest order coefficients $(n,m) \leq (1,1)$ are within reach for active compensation with the default MR-Open, even with yoke thicknesses down to 20 cm. The perturbations by the bending magnet on the higher order coefficients $\alpha_{20}, \alpha_{21}, \alpha_{30}, \alpha_{40}, \beta_{21}$ are in the 1-10 ppm range for a yoke thickness of 30 cm. Active compensation coils can be designed and added to the system to cancel these levels of perturbations.

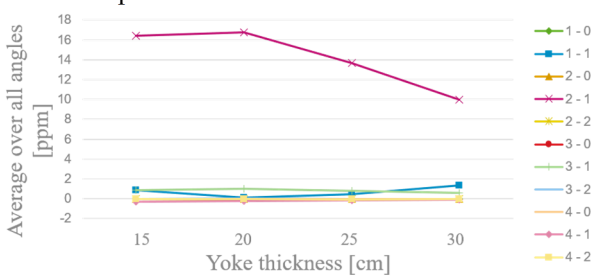

Figure 7: $\beta_{nm}^{\text{pert bend}}$ versus yoke thickness. The legend lists the $n-m$ parameters.

CONCLUSION

An option for the integration of a liquid helium free 0.5 T open MRI scanner based on the ASG MR-Open into an IBA ProteusONE PT gantry has been presented. An FEM analysis has been performed to assess the magnetic field perturbations by rotating ferromagnetic elements around the MRI, and by the fringe field of the 60° bending magnet mounted on the gantry.

The analysis shows that the rotations cause perturbations below the 50-ppm level, which can be actively compensated for with the default MR-Open system.

The bending magnet's fringe field causes perturbations, which cannot all be compensated for with the default MR-Open: With the maximum yoke thickness of 30 cm, nonlinear perturbations remain up to the 10-ppm level.

Consequently, in the synchronization of the operation of the MRI and the PT system, an image can be acquired simultaneously with the changing of the magnet's field only if active compensation coil sets are added to the system. Without these coils, image acquisition and changing magnet setpoints should be done successively. The two scenarios correspond to different trade-offs between treatment delivery speed and commissioning efforts.

REFERENCES

[1] B. Oborn *et al.*, "Future of medical physics: real-time MRI-guided proton therapy", *Med. Phys.*, vol. 44, no. 8, pp. e77-e90, Aug. 2017. doi:10.1002/mp.12371

[2] S. Schellhammer *et al.*, "Integrating a low-field open MR scanner with a static proton research beam line: proof of concept.", *Phys. Med. Bio.*, vol. 63, no. 23, p. 23LT01, Nov. 2018. doi:10.1088/1361-6560/aaece8

[3] E. Pearson *et al.*, "Magnet developments and commissioning for the IBA compact gantry", *IEEE Trans. App. Supercond.*, vol. 24, no. 3, p. 4401004, Jun. 2014. doi:10.1109/ TASC.2013.2284719

[4] ASG Superconductors – Paramed MRI Unit, https://www.paramedmedicalsystems.com/

[5] J. Marques *et al.*, "Low-field MRI: An MR physics perspective", *J. Magn. Reson. Imaging*, vol. 49, no. 6, p. 1528, Jun. 2019. doi:10.1002/jmri.26637

[6] Vector Fields Software, "OPERA Simulation Software", http://operafea.com

[7] Vector Fields Software Support, Klaus Hoffner, private communications, Dec. 2016.